Acta Geodyn. Geomater., Vol. 23, No. 3 (223), 393–402, 2026
DOI: 10.13168/AGG.2026.0026

journal homepage: https://www.irsm.cas.cz/acta

ORIGINAL PAPER

ASSESSING THE CONSISTENCY OF COASTAL SEA SURFACE HEIGHT MEASUREMENTS FROM SWOT ALTIMETRY AND TIDE GAUGES ALONG THE U.S. EAST COAST

Yuxuan FAN [1], Shunqiang HU [2], Lyubka PASHOVA [3], Xiwen SUN [4] and Xiaoxing HE [1] *

[1] *School of Airspace Technology, Jiangxi University of Science and Technology, Ganzhou, 341000, China*
[2] *Key Laboratory of Poyang Lake Wetland and Watershed Research, Ministry of Education, Jiangxi Normal University, Nanchang 330022, China*
[3] *National Institute of Geophysics, Geodesy and Geography – Bulgarian Academy of Sciences, Sofia, Bulgaria*
[4] *Jiangxi Polytechnic University, Jiujiang, 332007, China*

**Corresponding author's e-mail:* xxh@jxust.edu.cn

ARTICLE INFO

Article history:
Received 18 June 2026
Accepted 25 August 2026
Available online 7 September 2026

Keywords:
Surface Water and Ocean Topography
Sea Surface Height
Satellite Altimetry
Tide Gauge

ABSTRACT

In nearshore environments, the limited accuracy of traditional satellite altimetry in monitoring coastal sea-level changes restricts its application. The wide-swath, high-resolution measurements from the Surface Water and Ocean Topography (SWOT) satellite provide a new understanding of coastal sea-level variability. This study evaluates the capability of SWOT to observe the instantaneous sea surface height (SSH) along the U.S. East Coast between August 2023 and December 2025. The SWOT Level-2 KaRIn low-rate sea surface height expert data show good agreement with the results validated by tide gauges (TGs). In all pooled observations from the 12 TG stations, the Pearson correlation coefficient (R) between the SWOT and the TG measurements was 0.998, with a root mean square error (RMSE) of 0.295 m and a mean absolute error (MAE) of 0.224 m. These results demonstrate that, even under complex nearshore environmental conditions, the SWOT can effectively capture the SSH variability and exhibits considerable potential for coastal observations.

1. INTRODUCTION

The coastal regions are densely populated and highly vulnerable to global climate warming and sea-level rise (Nicholls and Mimura, 1998; Church et al., 2007; Kulp and Strauss, 2019; Roy et al., 2023; He et al., 2025). Therefore, accurate monitoring of sea-level variability is essential for coastal disaster prevention and sustainable socioeconomic development (Vinogradov and Ponte, 2011; Cazenave and Cozannet, 2014; Nicholls et al., 2014; Taherkhani et al., 2020; Liu et al., 2026). Tide gauges (TGs) have been used to monitor sea-level changes for more than three centuries and remain key reliable sources of coastal sea-level observations (Jevrejeva et al., 2014). Nevertheless, their global distribution is highly uneven, and their long-term records often contain temporal gaps (Cazenave et al., 2002; Wöppelmann et al., 2007; Vinogradov and Ponte, 2011; Bonaduce et al., 2016). Since 1993, satellite altimetry has become an important approach for monitoring global sea-level change, greatly improving the spatial coverage of sea-level observations (Cabanes et al., 2001; Ablain et al., 2017; Cazenave et al., 2018). In coastal regions, however, the accuracy of conventional satellite altimetry is significantly degraded compared to the open ocean because radar echo signals are strongly affected by complex coastal environments. As a result, obtaining high-precision coastal sea surface height (SSH) observations remains a long-standing challenge (Lago et al., 2017; Zhou et al., 2022). The implementation of the Surface Water and Ocean Topography (SWOT) mission provides new opportunities for improving coastal sea-level observations. In December 2022, the United States and France jointly launched the SWOT wide-swath altimetry mission. Equipped with the Ka-band Radar Interferometer (KaRIn), SWOT can provide two-dimensional SSH observations across two swaths approximately 50 km wide (Fu et al., 2024; Kacimi et al., 2025; Wang et al., 2025). In contrast to conventional altimetry satellites, which only acquire along-track measurements, the SWOT enables synchronous two-dimensional observations within the swath, thereby alleviating the limitations of traditional nadir-pointing sampling (Le Traon et al., 2019; Morrow et al., 2019; Bohé et al., 2025). This capability can reduce the impacts of temporal sampling inconsistencies and land contamination on altimetric accuracy (Kupavõh et al., 2025; Sun et al., 2026).

Several validation studies have been conducted to evaluate the SWOT's performance in sea-level monitoring. These multi-source investigations examined the consistency among SWOT, conventional satellite altimetry, and TG measurements (Chaudhary et al., 2025; Zhu et al., 2025). Further studies carried out in the Bristol Channel–Severn

Cite this article as: Fan Y, Hu S, Pashova L, Sun X, He X: Assessing the consistency of coastal sea surface height measurements from SWOT altimetry and tide gauges along the U.S. East Coast. Acta Geodyn. Geomater., 23, No. 3 (223), 393–402, 2026. DOI: 10.13168/AGG.2026.0026

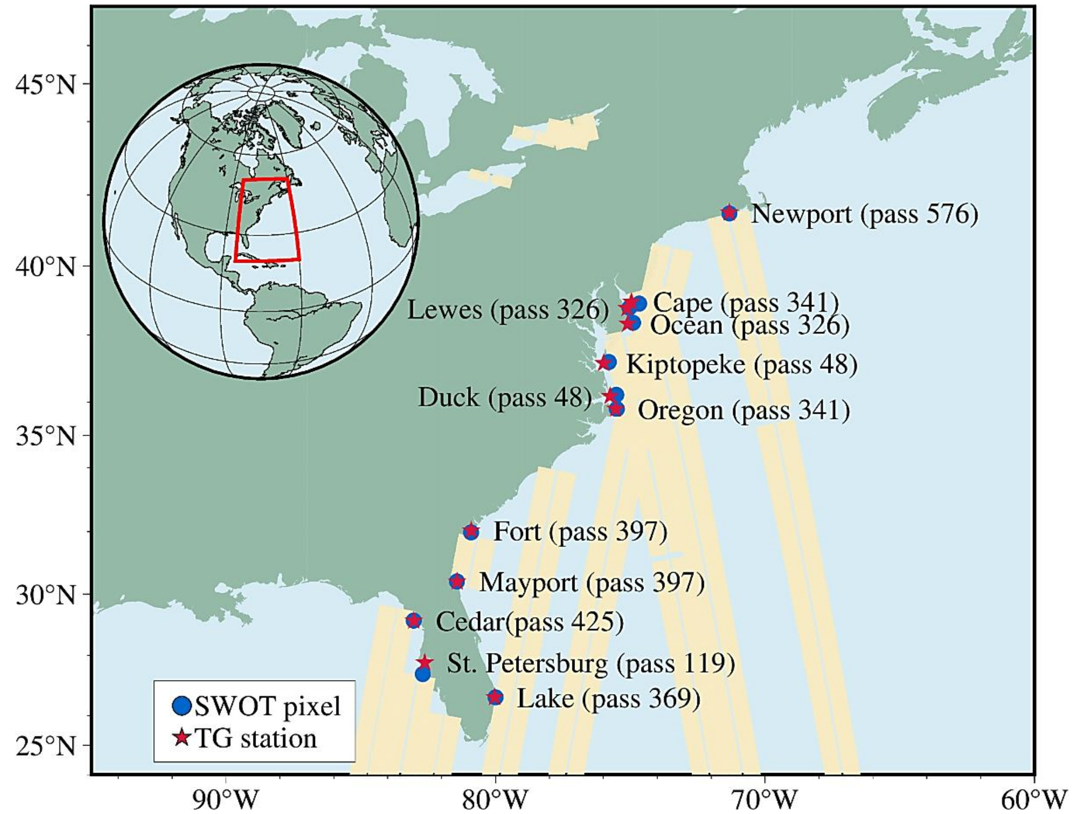

Fig. 1 Map of the study sites: the study area and a spatial distribution of the TG stations. Red dots denote the TG stations, while blue dots indicate the nearest satellite pixels corresponding to each TG station; the light orange stripes show the SWOT satellite tracks.

Estuary, the English Channel, and the coastal bays show that the SWOT can capture complex coastal sea-level variability and highly dynamic ocean processes (Hart-Davis et al., 2024; Lichtman et al., 2025; Turki et al., 2025; Vega-Gimenez et al., 2025; Rong et al., 2026). However, these studies were largely based on early Cal/Val phase data. As SWOT enters its 21-day repeat-science orbit, further assessments of its long-term ocean-monitoring performance are needed to provide more comprehensive and robust results.

The complex topography of the U.S. East Coast, influenced by the Gulf Stream and ocean dynamics, results in significant spatial variability in sea level (Piecuch et al., 2018; Chi et al., 2023; Piecuch and Beal, 2023), making it useful to assess the observing capability of SWOT in complex marine environments. In addition, many long-term operating TG stations provide reliable in situ observations, offering valuable reference data for validating SWOT SSH measurements. To the best of our knowledge, this is the first study conducted in the U.S. East Coast region to evaluate the accuracy of SWOT SSH observations. Approximately 40 science orbit cycles from 2023 to 2025 are used to assess SWOT's coastal SSH performance over an extended period. The remainder of the paper is organized as follows: the data and methods are presented in Section 2, the results are commented on in Section 3 and discussed in Section Section 4; and 5 contains the conclusions.

2. DATASETS AND METHODOLOGY

2.1. *TIDE GAUGE DATA*

The TG data used in this study are obtained from the Center for Operational Oceanographic Products and Services (CO-OPS) of the National Oceanic and Atmospheric Administration (NOAA) (https://tidesandcurrents.noaa.gov/, accessed on 15.02.2026). CO-OPS provides sea-level observations at a 6-min temporal resolution, with data quality ensured through automated processing and manual verification of the raw water level time series (Flick et al., 2003; Sweet et al., 2015). The TG stations were selected according to the following criteria: (1) quality-controlled 6-min water-level observations were available during the SWOT science-orbit period from August 2023 to December 2025; and (2) the selected stations represented a variety of coastal environments, including open ocean coasts, bay entrances, tidal inlets, and river estuaries. The spatial distribution of the selected TG stations is shown in Figure 1.

2.2. *SWOT SATELLITE ALTIMETRY DATA*

This study uses the SWOT Level 2 KaRIn low-rate ocean data products (SWOT_L2_KaRIn_SSH_Expert: https://doi.org/10.24400/527896/A01-2023.015, accessed on 15.02.2026). The product provides SSH observations on a 2 km × 2 km geographically fixed

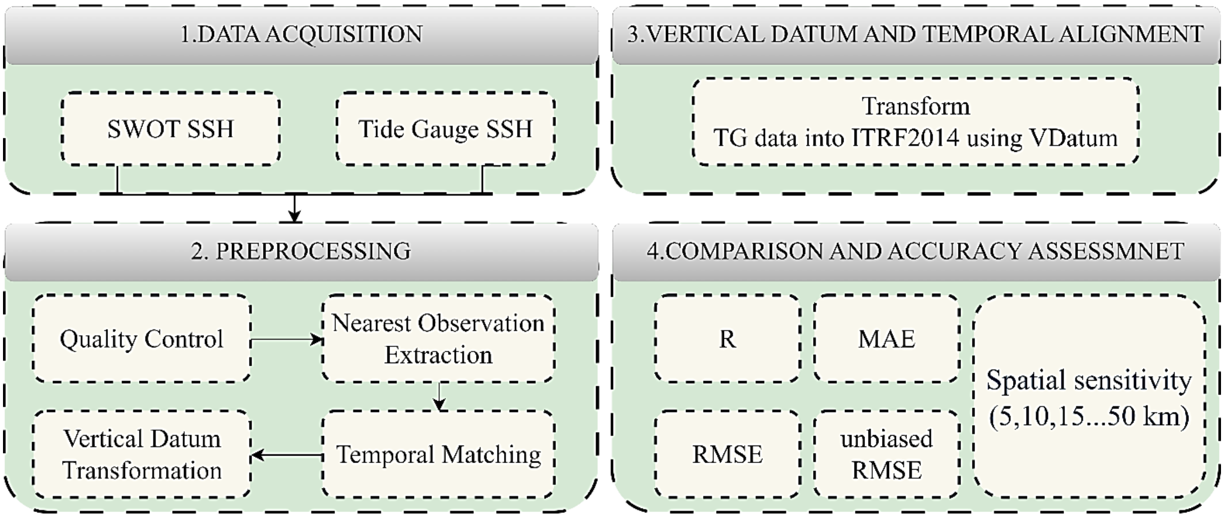

Fig. 2 Workflow for coastal SSH validation using SWOT and TG data, including quality control, spatial and temporal collocation, vertical-reference transformation, distance-weighted sensitivity analysis, and statistical evaluation.

grid. The science orbit has a 21-day repeat cycle, and the study period was from August 2023 to December 2025. The data product has been systematically corrected for major error sources, including dry and wet tropospheric delays, ionospheric delays, and sea-state bias. In addition, the SSH data are further corrected using the crossover calibration information provided in the product documentation (https://podaac.jpl.nasa.gov/dataset/SWOT_L2_LR_SSH_Expert_D, accessed on 15.02.2026).

2.3. EXPERIMENTAL WORKFLOW

The experiment consists of these main steps (Fig. 2): data acquisition, preprocessing and vertical datum transformation, and consistency assessment. The TG measurements serve as *in situ* references to evaluate the accuracy of the SWOT mission SSH data along the coast. The TG records were quality-controlled and manually verified by NOAA, whereas the SWOT observations were screened according to the quality flags provided with the product. The distances between each TG station and all SWOT pixels were calculated for each SWOT overpass. Pixels with missing SSH values and those that did not pass the quality control were excluded, and the nearest remaining valid pixel was selected for comparison. Table 1 lists the nearest SWOT pass associated with each TG station and the corresponding distance. The TG water level was linearly interpolated from the two valid 6-min bracketing observations to the exact SWOT observation time, using the millisecond-resolution data acquisition time of each selected SWOT pixel as a reference. Each matched pair represented one valid overpass within the 21-day SWOT science-orbit repeat cycle. Using the vertical datum (VDatum) transformation tool, the TG observations were transformed to an ellipsoidal height reference frame consistent with that of the SWOT SSH measurements (https://vdatum.noaa.gov/; accessed on 15.03.2026). VDatum provides location-dependent transformations among tidal datums, orthometric vertical datums, and ellipsoidal height reference systems. In this study, the VDatum of the GEOID18 geoid model was used to convert NAVD88 orthometric heights to ellipsoidal heights in the NAD83(2011) reference frame. The resulting NAD83(2011) ellipsoidal coordinates were then transformed to the ITRF2014 reference frame using NOAA's Horizontal Time-Dependent Positioning model. After the reference-frame transformation, vertical land motion (VLM) corrections were applied to the TG ellipsoidal heights using GNSS-derived VLM rates provided by the Nevada Geodetic Laboratory (https://geodesy.unr.edu/vlm.php):

$$h_{\mathrm{TG,corr}}(t) = h_{\mathrm{TG}}{}^{\mathrm{ITRF2014(2010.0)}}(t) + \frac{v}{1000}(t - 2010.0) \quad (1)$$

where $h_{\mathrm{TG,corr}}(t)$ is the VLM-corrected TG ellipsoidal height at observation epoch t, $h_{\mathrm{TG}}{}^{\mathrm{ITRF2014(2010.0)}}(t)$ is the TG water level transformed from a NAVD88-referenced orthometric height into an ITRF2014 ellipsoidal height using VDatum and the Horizontal Time-Dependent Positioning model, t is the observation epoch expressed as a decimal year, and v is the VLM rate in mm/yr, with positive values indicating uplift. The factor 1000 converts millimeters to meters.

Agreement between the two datasets was evaluated using the Pearson correlation coefficient (R), mean absolute error (MAE), root mean square error (RMSE), and unbiased root mean square error (unbiased RMSE):

$$R = \frac{\sum_{i=1}^{N}(y_i - \bar{y})(\hat{y}_i - \bar{\hat{y}})}{\sqrt{\sum_{i=1}^{N}(y_i - \bar{y})^2 \sum_{i=1}^{N}(\hat{y}_i - \bar{\hat{y}})^2}} \quad (2)$$

Table 1 Locations of TG stations and their nearestt SWOT passes and vertical land motion rates.

TG Station	TG ID	Longitude (°)	Latitude (°)	SWOT Pass	Distance (km)	VLM (mm/yr)
Cape May	8536110	-74.960°	38.968°	341	25.57	-2.001±0.281
Cedar Key	8727520	-83.031°	29.134°	425	2.97	-0.653±0.357
Duck	8651370	-75.747°	36.183°	48	20.85	-2.019±0.300
Fort Pulaski	8670870	-80.903°	32.034°	397	27.51	-0.862±0.305
Kiptopeke	8632200	-75.988°	37.167°	48	17.65	-1.843±0.432
Lake Worth Pier	8722670	-80.034°	26.613°	369	3.99	-0.337±0.351
Lewes	8557380	-75.119°	38.783°	326	7.89	-2.117±0.282
Mayport	8720218	-81.428°	30.398°	397	1.06	-0.763±0.406
Newport	8452660	-71.327°	41.505°	576	4.35	-0.605±0.333
Ocean City Inlet	8570283	-75.092°	38.328°	326	17.13	-2.506±0.237
Oregon Inlet Marina	8652587	-75.548°	35.795°	341	4.53	-2.231±0.430
St. Petersburg	8726520	-82.627°	27.761°	119	46.90	-0.914±0.370

Table 2 Pearson correlation coefficient and statistical metrics (m) of the comparison between SSH observations from 12 TG stations and the nearest SWOT pixels. The difference was defined as the TG SSH minus the corresponding SWOT SSH.

TG Station	R	RMSE	MAE	Unbiased RMSE	Min Diff	Max Diff	Mean Diff
Cape	0.922	0.336	0.277	0.246	-0.218	0.774	0.229
Cedar	0.931	0.190	0.150	0.190	-0.408	0.480	0.011
Duck	0.950	0.194	0.162	0.142	-0.463	0.177	-0.133
Fort	0.948	0.354	0.262	0.258	-0.829	0.107	-0.243
Kiptopeke	0.870	0.247	0.197	0.192	-0.261	0.598	0.155
Lake	0.891	0.292	0.266	0.148	-0.121	0.499	0.252
Lewes	0.960	0.146	0.108	0.138	-0.296	0.374	0.046
Mayport	0.867	0.459	0.377	0.270	-1.045	0.079	-0.371
Newport	0.688	0.308	0.212	0.297	-1.046	0.338	-0.083
Ocean	0.927	0.185	0.162	0.162	-0.402	0.306	-0.091
Oregon	0.726	0.251	0.199	0.249	-0.509	0.554	0.026
St. Petersburg	0.614	0.412	0.325	0.286	-1.375	0.199	-0.297

$$RMSE = \sqrt{\frac{1}{N}\sum_{i=1}^{N}(y_i - \hat{y}_i)^2} \tag{3}$$

$$\text{MAE} = \frac{1}{N}\sum_{i=1}^{N}|y_i - \hat{y}_i| \tag{4}$$

$$\text{unbiased RMSE} = \sqrt{\frac{1}{N}\sum_{i=1}^{N}\left[(y_i - \bar{y}) - (\hat{y}_i - \bar{\hat{y}})\right]^2} \tag{5}$$

where y_i denotes the i -th TG observation,$\hat{y}_i$ denotes the corresponding SWOT observation, $\bar{y}$and $\bar{\hat{y}}$ denote the mean SSH of the TG and SWOT observations, respectively, and $N$is the total number of matched observation pairs.

3. RESULTS

Table 2 summarizes the R, RMSE, MAE, unbiased RMSE, maximum, minimum, and mean differences between the SSH observations from the 12 TG stations and their nearest valid SWOT pixels. Figure 3 shows the SSH time series from the TG and the SWOT observations at multiple stations. Overall, the SWOT results agree well with the TG measurements, with station-specific RMSEs of 0.146–0.459 m and MAEs of 0.108–0.377 m. Both datasets capture coherent coastal SSH fluctuations, indicating that the SWOT successfully resolves the dominant sea-level variability during the observation period. Linear regression analysis of data from all stations (Fig. 4) shows that most scatter points cluster around the 1:1 reference line. The pooled SWOT and TG observations yield an overall R of 0.998 and an RMSE

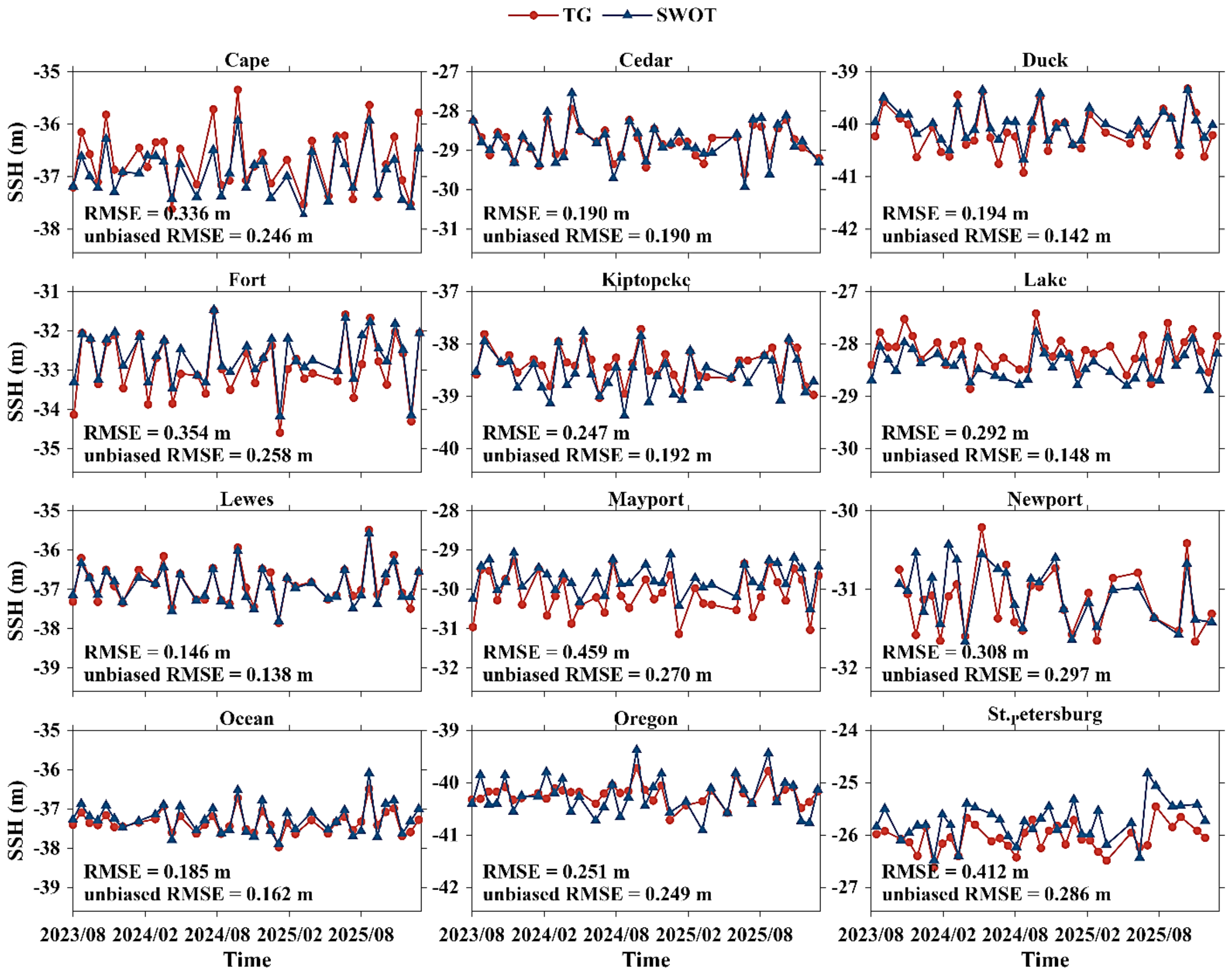

Fig. 3 Comparison of the SSH time series from the SWOT and the 12 TG stations from August 2023 to December 2025. Each matched data pair represents one valid SWOT overpass within the 21-day repeat cycle.

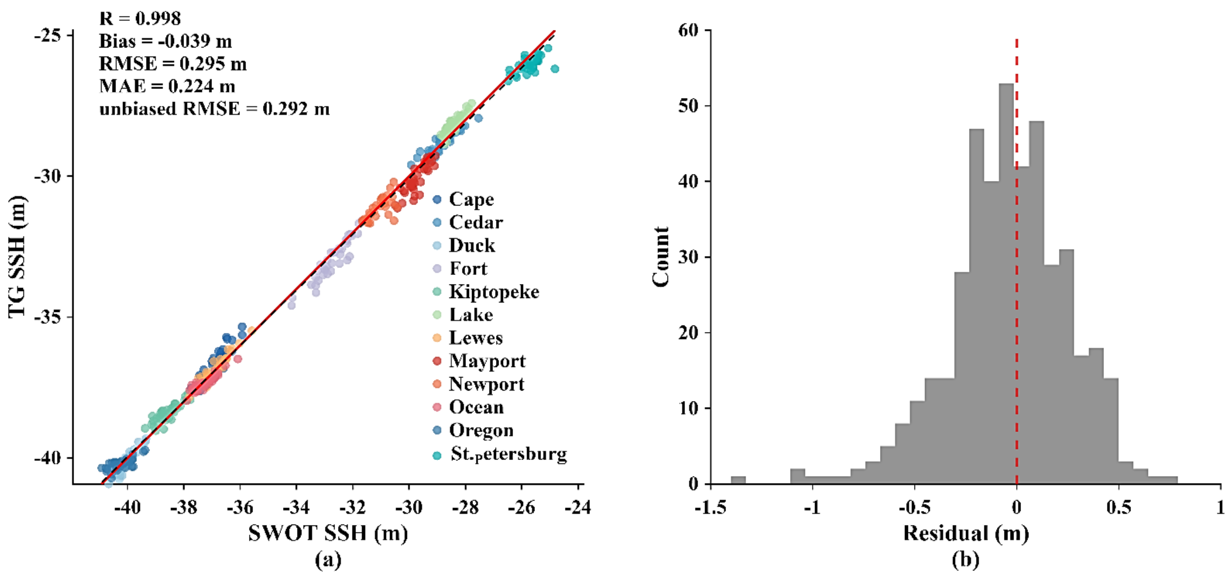

Fig. 4 Comparison of the matched SWOT and the TG SSH observations at 12 stations (a) and a histogram of the distribution of TG–SWOT residuals (b). Bias is the signed mean difference.

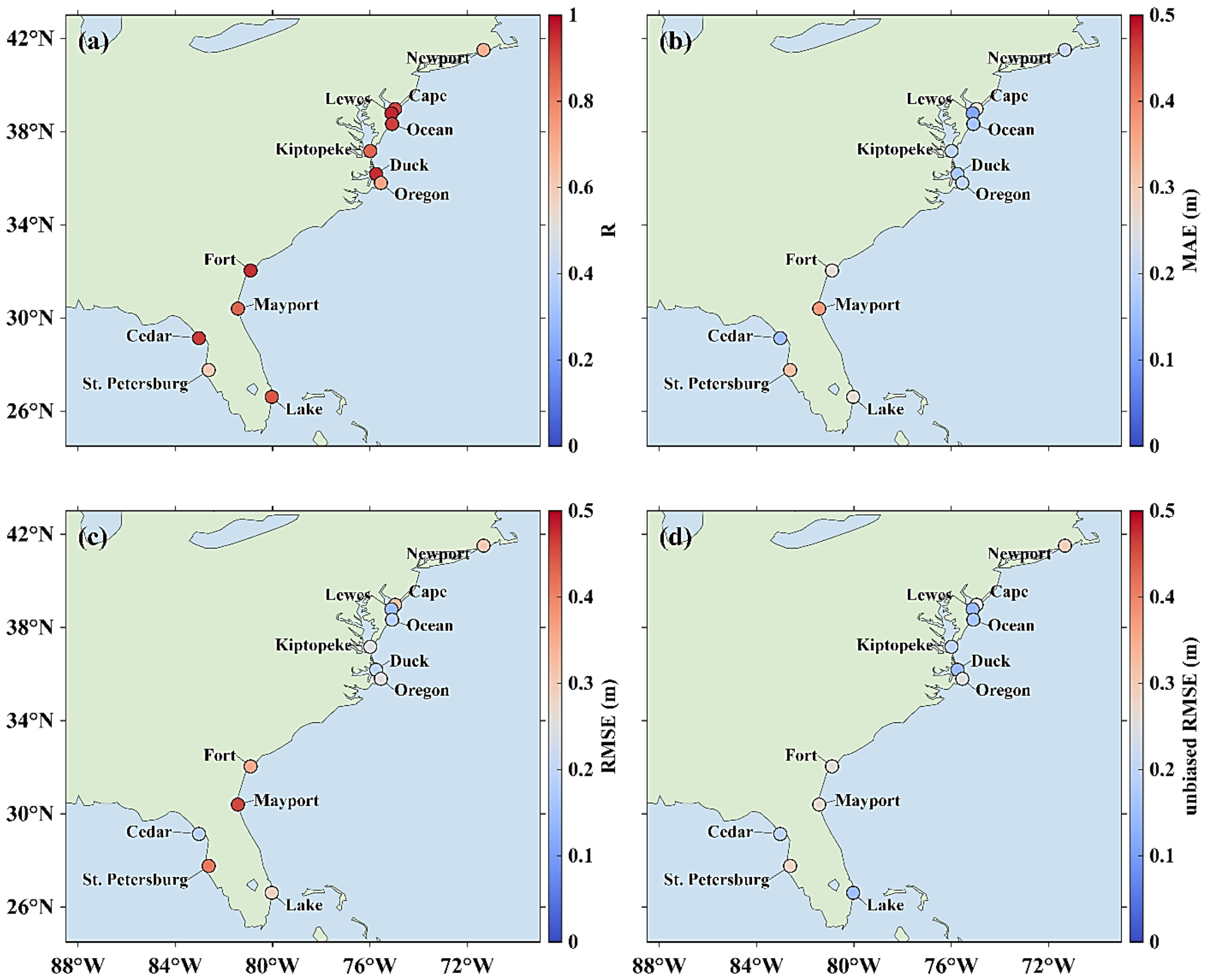

Fig. 5 Spatial distribution of agreement metrics between the 12 TG stations and their nearest SWOT pixels.

of 0.295 m. In addition, most residuals fall within ±0.5 m, demonstrating the overall reliability of the SWOT SSH measurements in coastal regions.

Although the overall SSH agreement across the region is high, notable differences remain among the stations. Figures 5 and 6 show the spatial distribution of station performance indicators and their relationships with distance, respectively. The Mayport station is located only 1.06 km from the nearest SWOT pixel; however, the MAE and RMSE are 0.377 and 0.459 m, respectively. After removing the mean difference, the unbiased RMSE is 0.270 m, indicating a notable mean offset within the total error. Furthermore, the Mayport station is located in the lower estuary of the St. Johns River, where the mean tidal range is approximately 4.5 ft (~1.37 m). Driven by semidiurnal tides, the tidal reversals are accompanied by significant mixing of saltwater and freshwater and strong salinity-driven density gradients (Bellino and Spechler, 2013). These complex local conditions may produce strong spatial variability, causing nearby SWOT pixels and the TG observations to collect different water-level signals.

At the St. Petersburg station, the nearest valid SWOT pixel is approximately 46.90 km away. The MAE and RMSE are 0.325 and 0.412 m, respectively, with an unbiased RMSE of 0.286 m after removing the mean difference. This TG is located at a port within Tampa Bay (Goodwin, 1987). Hydrodynamic studies indicate that Tampa Bay exhibits distinct tidal circulation and transport characteristics, with significant spatial variations in circulation intensity between different parts of the bay. Consequently, a SWOT pixel located approximately 46.90 km away may represent a different region of the bay and be associated with a distinct hydrodynamic environment. These results demonstrate that multiple factors influence the differences between the TG and the SWOT observations. First, satellite altimetry observations in coastal areas are still affected by land and complex coastal environments (Vignudelli et al., 2019; Gómez-Enri et al., 2026); second, vertical datum transformations may introduce uncertainties in TG measurements. In addition, the nearest-neighbor matching approach may introduce representativeness errors, given that the distances between the TG stations and their corresponding SWOT pixels vary from approximately 1 to 50 km. Despite these sources of uncertainty, the strong agreement in temporal variability between the SWOT and the TG suggests

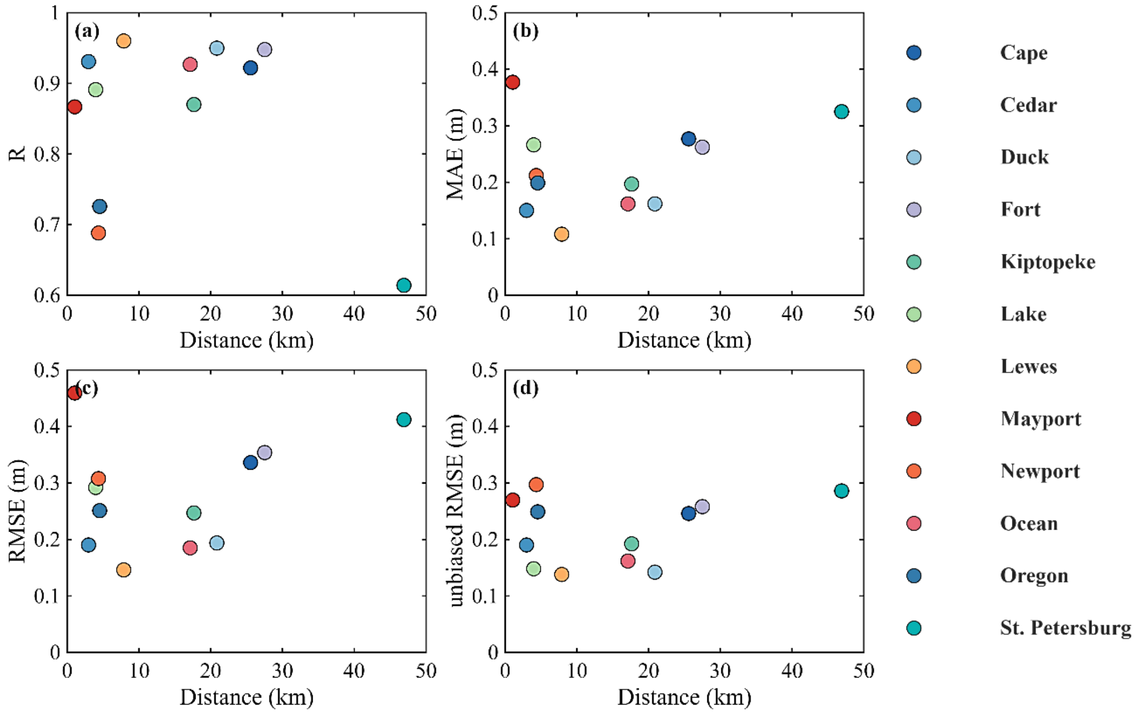

Fig. 6 Variations in the agreement metrics between the TG and the SWOT SSH observations at the 12 stations with distance. The horizontal axis represents the distance between each TG station and its nearest quality-controlled SWOT pixel.

that the SWOT effectively captures the dominant variability of instantaneous coastal SSH, highlighting its capability to monitor complex dynamic nearshore environments.

4. DISCUSSION

To assess the spatial representativeness errors that may be introduced by nearest-neighbor matching, we conducted a distance-weighted spatial sensitivity analysis. For each TG station and valid SWOT overpass, quality-controlled SWOT pixels within search radii of 5, 10, 15, 20, 30, 40, and 50 km around the TG station were extracted, and the mean SSH was calculated using inverse-distance weighting. The weighted-average results at each radius were compared to the SSH obtained from the nearest valid SWOT pixel, and the evaluation metrics were analyzed in terms of how they varied with changing radius.

Figure 7 shows the variations in the Pearson correlation coefficient and error metrics between the TG and the weighted SWOT SSH, varying over search radii of 5–50 km. The RMSE and unbiased RMSE at the Cedar, Ocean, and Oregon stations showed little variation with radius. In contrast, the Fort, Lewes, and Newport stations exhibit relatively high R values and low errors at a radius of 10–20 km. When the radius exceeds 30 km, the errors at Lake and Fort stations increase substantially. This behavior may arise because more distant SWOT pixels represent different coastal hydrodynamic conditions, thereby increasing errors in spatial representativeness. At several stations, the unbiased RMSE is substantially lower than the corresponding RMSE, particularly at larger radii. For example, at the Mayport station, the RMSE reaches 1.757 m at a radius of 20 km, whereas the unbiased RMSE is only 0.295 m. At Lake station, as the radius increases from 5 km to 50 km, the RMSE rises from 0.257 to 0.984 m, while the unbiased RMSE increases only slightly from 0.135 to 0.162 m. This suggests that the increase in total error with radius may be partly attributed to a growing mean offset between the weighted SWOT SSH and the TG observations.

Figure 8 depicts a comparison of the evaluation metrics obtained using inverse-distance weighting with those obtained by the nearest-pixel method. For each station–radius combination, the two methods were evaluated using the same TG observations and SWOT overpasses. At the Fort station, agreement metrics improved within the 10–20 km radius range, though some metrics were inferior to the nearest-pixel method at larger radii. At the Mayport and Lake stations, the absolute biases and RMSE produced by the distance-weighted method were larger than those of the nearest-pixel method across most radii. While larger radii allow the inclusion of more valid SWOT pixels, an excessively large search area may incorporate pixels affected by different coastal conditions, bathymetric variability, and SSH gradients, thereby increasing spatial representativeness errors. At radii of 15–30 km, the inverse-distance weighting reduces the standard deviation of the TG–SWOT differences at the Fort, Newport, and Oregon stations, indicating reduced

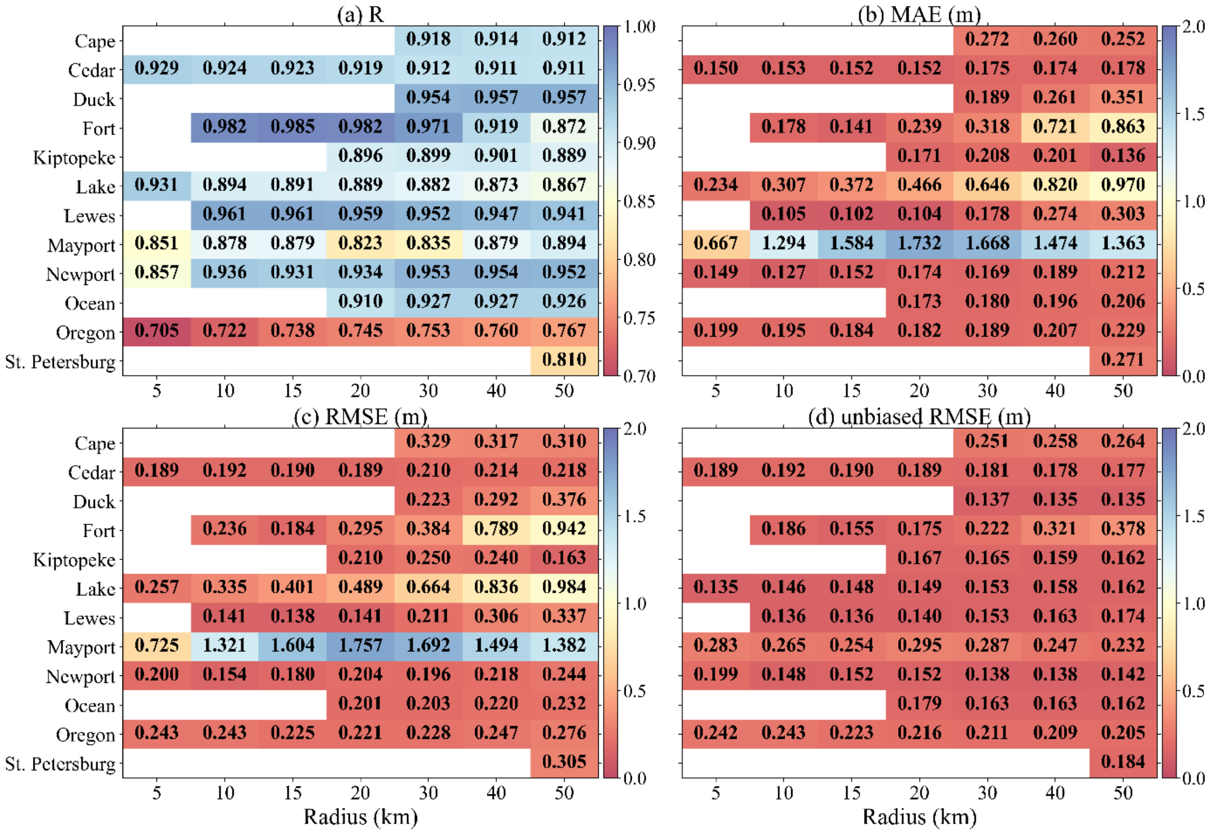

Fig. 7 Radius dependence of agreement metrics between the TG and the inverse-distance weighting SWOT SSH. Blank cells indicate insufficient valid matched observations.

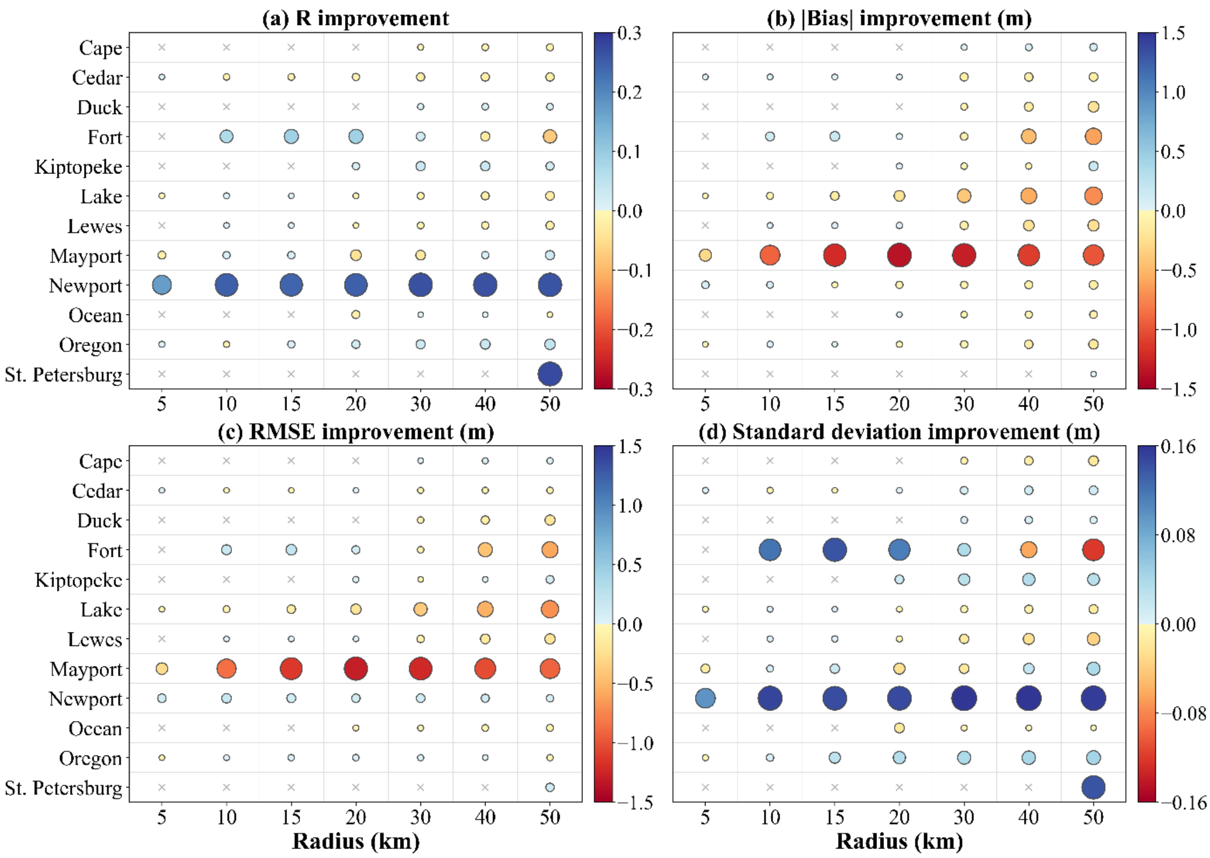

Fig. 8 Changes in evaluation metrics for inverse-distance weighting relative to nearest-pixel matching across search radii. Blue and red bubbles indicate improvement and deterioration, respectively, and bubble size represents the magnitude of change. Crosses indicate cases with no common valid observations.

residual dispersion and possibly reduced sensitivity to the individual-pixel noise. Overall, expanding the search radius does not universally improve matching accuracy, as the optimal spatial matching scale depends on the availability of valid SWOT observations and the local coastal environment near each station.

5. CONCLUSION

This study evaluates the capability of the SWOT mission to observe the SSH along the U.S. East Coast covering approximately 40 21-day repeat cycles from August 2023 to December 2025. Comparisons made with the 12 TG observations show that the SWOT effectively captures SSH variability and demonstrates strong consistency across multiple stations. These results demonstrate SWOT's capability in complex coastal environments and highlight its potential to support high-resolution investigations of sea surface height variability. Future work should further integrate multi-source observations to more comprehensively assess SWOT's applicability in complex coastal environments, thereby improving the accuracy and reliability of nearshore ocean monitoring and supporting better regional and local-scale studies of ocean dynamics.

ACKNOWLEDGMENT

This work was sponsored by the National Natural Science Foundation of China (42364002) and the Natural Science Foundation of Jiangxi Province (20252BAC220015).

REFERENCES

Ablain, M., Legeais, J.F., Prandi, P., Marcos, M., Fenoglio-Marc, L., Dieng, H.B., Benveniste, J. and Cazenave, A.: 2017, Satellite altimetry-based sea level at global and regional scales. In: Cazenave, A., Champollion, N., Paul, F. and Benveniste, J. (eds), Integrative study of the mean sea level and its components. Space Sciences Series of ISSI, 58, 9–33. Springer, Cham. DOI: 10.1007/s10712-016-9389-8

Bellino, J.C., and Spechler, R.M.: 2013, Potential effects of deepening the St. Johns River navigation channel on saltwater intrusion in the surficial aquifer system, Jacksonville, Florida. U.S. Geological Survey Scientific Investigations Report., 2013–5146. DOI: 10.3133/sir20135146

Bohé, A., Chen, A., Chen, C., Dubois, P., Fore, A., Molero, B., Peral, E., Raynal, M., Stiles, B. and Ardhuin, F.: 2025, Measuring significant wave height fields in two dimensions at kilometric scales with SWOT. IEEE Trans. Geosci. Remote Sens., 63, 1–19. DOI: 10.1109/TGRS.2025.3551605

Bonaduce, A., Pinardi, N., Oddo, P., Spada, G. and Larnicol, G.: 2016, Sea-level variability in the Mediterranean Sea from altimetry and tide gauges. Clim. Dyn., 47, 9, 2851-2866. DOI: 10.1007/s00382-016-3001-2

Cabanes, C., Cazenave, A. and Le Provost, C.: 2001, Sea level rise during past 40 years determined from satellite and in situ observations. Science., 294, 5543, 840–842. DOI: 10.1126/science.1063556

Cazenave, A., Bonnefond, P., Mercier, F., Dominh, K. and Toumazou, V.: 2002, Sea level variations in the Mediterranean Sea and Black Sea from satellite altimetry and tide gauges. Glob. Planet. Change., 34, 1-2, 59–86. DOI: 10.1016/S0921-8181(02)00106-6

Cazenave, A. and Cozannet, G.L.: 2014, Sea level rise and its coastal impacts. Earth's Future., 2, 2, 15–34. DOI: 10.1002/2013EF000188

Cazenave, A., Palanisamy, H. and Ablain, M.: 2018, Contemporary sea level changes from satellite altimetry: What have we learned? What are the new challenges? Adv. Space Res., 62, 7, 1639–1653. DOI: 10.1016/j.asr.2018.07.017

Chaudhary, A., Chander, S., Surisetty, A.K., Agrawal, R., Agarwal, N., Gupta, P.K., Kumar, R., Sharma, R., Shesu, R.V. and Bhaskar, T.V.S.U.: 2025, Evaluation of SWOT Beta geophysical products in the Indian region during CAL-VAL Phase over the land and oceans. J. Indian Soc. Remote Sens., 53, 12, 4123–4136. DOI: 10.1007/s12524-025-02237-5

Chi, L., Wolfe, C.L.P. and Hameed, S.: 2023, Reconsidering the relationship between Gulf Stream transport and dynamic sea level at U.S. East Coast. Geophys. Res. Lett., 50, 9, e2022GL102018. DOI: 10.1029/2022GL102018

Church, J., Wilson, S., Woodworth, P. and Aarup, T.: 2007, Understanding sea level rise and variability. Eos, Trans. Am. Geophys. Union, 88, 4. DOI: 10.1029/2007EO040008

Flick, R.E., Murray, J.F. and Ewing, L.C.: 2003, Trends in United States tidal datum statistics and tide range. J. Waterw. Port Coast. Ocean Eng., 129, 4, 155–164. DOI: 10.1061/(ASCE)0733-950X(2003)129:4(155)

Fu, L.L., Pavelsky, T., Cretaux, J.F., Morrow, R., Farrar, J.T., Vaze, P., Sengenes, P., Vinogradova‐Shiffer, N., Sylvestre‐Baron, A. and Picot, N.: 2024, The surface water and ocean topography mission: A breakthrough in radar remote sensing of the ocean and land surface water. Geophys. Res. Lett., 51, 4, e2023GL107652. DOI: 10.1029/2023GL107652

Gómez-Enri, J., Arribas-Rodríguez, B., Tejedor, B., Álvarez, O., González, C.J. and Vignudelli, S.: 2026, Validation of the Surface Water and Ocean Topography (SWOT) KaRIn Sea Level Data. IEEE Trans. Geosci. Remote Sens., 64, 1–11. DOI: 10.1109/TGRS.2026.3679467

Goodwin, C.R.: 1987, Tidal-flow, circulation, and flushing changes caused by dredge and fill in Tampa Bay, Florida. U.S. Geological Survey Water-Supply Paper, 2282. DOI: 10.3133/wsp2282

Hart‐Davis, M.G., Andersen, O.B., Ray, R.D., Zaron, E.D., Schwatke, C., Arildsen, R.L., Dettmering, D. and Nielsen, K.: 2024, Tides in complex coastal regions: Early case studies from wide‐swath SWOT measurements. Geophys. Res. Lett., 51, 20, e2024GL109983. DOI: 10.1029/2024GL109983

He, X., Huang, J., Montillet, J.P., Wang, S., Kermarrec, G., Shum, C.K., Hu, S. and Wang, F.: 2025, A noise reduction approach for improve North American regional sea level change from satellite and in situ observations. Surv. Geophys. DOI: 10.1007/s10712-025-09894-8

Jevrejeva, S., Moore, J.C., Grinsted, A., Matthews, A.P. and Spada, G.: 2014, Trends and acceleration in global and regional sea levels since 1807. Glob. Planet. Change., 113, 11–22. DOI: 10.1016/j.gloplacha.2013.12.004

Kacimi, S., Jaruwatanadilok, S. and Kwok, R.: 2025, SWOT observations over sea ice: A first look. Geophys. Res. Lett., 52, 10, e2025GL116079. DOI: 10.1029/2025GL116079

Kulp, S.A. and Strauss, B.H.: 2019, New elevation data triple estimates of global vulnerability to sea-level rise and coastal flooding. Nat. Commun., 10, 1, 4844. DOI: 10.1038/s41467-019-12808-z

Kupavõh, A., Delpeche-Ellmann, N., Ellmann, A. and Soomere, T.: 2025, Examining the performance of satellite altimetry (SWOT) sea level data in the coastal areas of the Baltic Sea. J. Coast. Res., 113, SI, 534–538. DOI: 10.2112/JCR-SI113-105.1

Lago, L.S., Saraceno, M., Ruiz-Etcheverry, L.A., Passaro, M., Oreiro, F.A., D'Onofrio, E.E. and González, R.A.: 2017, Improved sea surface height from satellite altimetry in coastal zones: A case study in Southern Patagonia. IEEE J. Sel. Top. Appl. Earth Obs. Remote Sens., 10, 8, 3493–3503. DOI: 10.1109/JSTARS.2017.2694325

Le Traon, P.Y., Reppucci, A., Alvarez Fanjul, E., Aouf, L., Behrens, A., Belmonte, M., Bentamy, A., Bertino, L., Brando, V.E. and Kreiner, M.B.: 2019, From observation to information and users: The Copernicus Marine Service perspective. Front. Mar. Sci., 6, 234. DOI: 10.3389/fmars.2019.00234

Lichtman, I.D., Bell, P.S., Gommenginger, C., Banks, C., Calafat, F.M., Brown, J. and Williams, S.D.P.: 2025, Evaluating water levels from the surface water and ocean topography (SWOT) mission in a hyper‐tidal coastal and estuarine environment. Earth Space Sci., 12, 7, e2024EA004104. DOI: 10.1029/2024EA004104

Liu, H., Wang, S., Pashova, L., Zhang, Z., He, X., Dong, J., Li, G. and Xiao, M.: 2026, A multiscale GR-EOF approach reveals climate mode biases in sea level rise estimates. Appl. Ocean Res., 174, 105190. DOI: 10.1016/j.apor.2026.105190

Morrow, R., Fu, L.-L., Ardhuin, F., Benkiran, M., Chapron, B., Cosme, E., d'Ovidio, F., Farrar, J.T., Gille, S.T. and Lapeyre, G.: 2019, Global observations of fine-scale ocean surface topography with the surface water and ocean topography (SWOT) mission. Front. Mar. Sci., 6, 232. DOI: 10.3389/fmars.2019.00232

Nicholls, R.J., Hanson, S.E., Lowe, J.A., Warrick, R.A., Lu, X. and Long, A.J.: 2014, Sea‐level scenarios for evaluating coastal impacts. WIREs Clim. Chang., 5, 1, 129–150. DOI: 10.1002/wcc.253

Nicholls, R.J. and Mimura, N.: 1998, Regional issues raised by sea-level rise and their policy implications. Clim. Res., 11, 5–18. DOI: 10.3354/cr011005

Piecuch, C.G. and Beal, L.M.: 2023, Robust weakening of the Gulf Stream during the past four decades observed in the Florida Straits. Geophys. Res. Lett., 50, 18, e2023GL105170. DOI: 10.1029/2023GL105170

Piecuch, C.G., Huybers, P., Hay, C.C., Kemp, A.C., Little, C.M., Mitrovica, J.X., Ponte, R.M. and Tingley, M.P.: 2018, Origin of spatial variation in U.S. East Coast sea-level trends during 1900–2017. Nature, 564, 7736, 400–404. DOI: 10.1038/s41586-018-0787-6

Rong, Y., Bates, P., Neal, J., Bell, P., Gommenginger, C., Lichtman, I.D., Banks, C., Calafat, F.J.M., Martin, A. and Brown, J.: 2026, Evaluating SWOT in the coastal zone: Comparisons with tide gauge and airborne LiDAR in the Bristol Channel and Severn Estuary, UK. Geophys. Res. Lett., 53, 2, e2025GL116590. DOI: 10.1029/2025GL116590

Roy, P., Pal, S.C., Chakrabortty, R., Chowdhuri, I., Saha, A. and Shit, M.: 2023, Effects of climate change and sea-level rise on coastal habitat: Vulnerability assessment, adaptation strategies and policy recommendations. J. Environ. Manag., 330, 117187. DOI: 10.1016/j.jenvman.2022.117187

Sun, H., Jin, T., Li, J., Xian, H. and Shi, J.: 2026, Mitigating errors in marine gravity recovery induced by sea level variability in SWOT observations. Int. J. Appl. Earth Obs. Geoinf., 146, 105027. DOI: 10.1016/j.jag.2025.105027

Sweet, W.V., Park, J., Gill, S. and Marra, J.: 2015, New ways to measure waves and their effects at NOAA tide gauges: A Hawaiian‐network perspective. Geophys. Res. Lett., 42, 21, 9355–9361. DOI: 10.1002/2015GL066030

Taherkhani, M.,Vitousek, S., Barnard, P.L., Frazer, N., Anderson, T.R. and Fletcher, C.H.: 2020, Sea-level rise exponentially increases coastal flood frequency. Sci. Rep., 10, 1, 6466. DOI: 10.1038/s41598-020-62188-4

Turki, E.I., Islam, M.S., Solano, C.L., Salameh, E., Domingues, M., Mendoza, T., Aouf, L., Froideval, L., Barcelo, D.G. and Laignel, B.: 2025, On the use of SWOT altimetry data for monitoring coastal hydrodynamics. Int. J. Appl. Earth Obs. Geoinf., 145, 104982. DOI: 10.1016/j.jag.2025.104982

Vega‐Gimenez, D., Amores, A., Paris, A. and Pascual, A.: 2025, Expanding the coastal observation frontier: SWOT reveals the spatial footprint of storm surges. Geophys. Res. Lett., 52, 24, e2025GL117299. DOI: 10.1029/2025GL117299

Vignudelli, S., Birol, F., Benveniste, J., Fu, L.-L., Picot, N., Raynal, M. and Roinard, H.: 2019, Satellite altimetry measurements of sea level in the coastal zone. Surv. Geophys., 40, 6, 1319–1349. DOI: 10.1007/s10712-019-09569-1

Vinogradov, S.V. and Ponte, R.M.: 2011, Low‐frequency variability in coastal sea level from tide gauges and altimetry. J. Geophys. Res., Oceans, 116, C7. DOI: 10.1029/2011JC007034

Wang, J., Lucas, A.J., Stalin, S., Lankhorst, M., Send, U., Schofield, O., Kachelein, L., Haines, B., Meinig, C. and Pinkel, R.: 2025, SWOT mission validation of sea surface height measurements at sub‐100 km scales. Geophys. Res. Lett., 52, 11, e2025GL114936. DOI: 10.1029/2025GL114936

Wöppelmann, G., Miguez, B.M., Bouin, M.N. and Altamimi, Z.: 2007, Geocentric sea-level trend estimates from GPS analyses at relevant tide gauges world-wide. Glob. Planet. Change, 57, 3-4, 396–406. DOI: 10.1016/j.gloplacha.2007.02.002

Zhou, D., Liu, Y., Feng, Y., Zhang, H., Fu, Y., Liu, Y. and Tang, Q.: 2022, Absolute sea level changes along the coast of China from tide gauges, GNSS, and satellite altimetry. J. Geophys. Res., Oceans, 127, 9, e2022JC018994. DOI: 10.1029/2022JC018994

Zhu, H., Peng, F. and Shen, Y.: 2025, Validation of sea level anomalies from the SWOT altimetry mission around the Coastal Regions of East Asia and the U.S. West Coast. Water, 17, 21, 3066. DOI: 10.3390/w17213066